Nano World Journal

https://doi.org/10.17756/nwj.2023-s3-127

Research Article

Open Access

Transforming Fuel Efficiency with Silicon Dioxide Nanoparticles: Insights into Improved Spray Behavior and Physical Parameters

Megha Pandey[1], Surulivelrajan Tharmarajapandian[2*], I. B. Sapaev[3], Mohammed I. Habelalmateen[4] and Mangayarkarasi[5]

[1]*Christ (Deemed to be University), Bengaluru, Karnataka, India*

[2]*Department of Mechanical Engineering, Prince Shri Venkateshwara Padmavathy Engineering College, Chennai, Tamil Nadu, India*

[3]*Head of the department Physics and Chemistry, Tashkent Institute of Irrigation and Agricultural Mechanization Engineers, National Research University, Tashkent, Uzbekistan, Western Caspian University, Scientific researcher, Baku, Azerbaijan*

[4]*Department of Physics and Chemistry, School of Engineering, Central Asian University, Tashkent, Uzbekistan*

[5]*The Islamic University, Najaf, Iraq*

[6]*Department of Electronics and Communication Engineering, New Prince Shri Bhavani College of Engineering, Chennai, Tamil Nadu, India*

[*]Correspondence to:
Surulivelrajan Tharmarajapandian
Department of Mechanical Engineering,
Prince Shri Venkateshwara Padmavathy Engineering College,
Chennai, Tamil Nadu, India.
E-mail: surulivelt@gmail.com

Received: July 28, 2023
Accepted: October 27, 2023
Published: October 31, 2023

Citation: Pandey M, Tharmarajapandian S, Sapaev IB, Habelalmateen MI, Mangayarkarasi. 2023. Transforming Fuel Efficiency with Silicon Dioxide Nanoparticles: Insights into Improved Spray Behavior and Physical Parameters. *NanoWorld J* 9(S3): S714-S720.

Copyright: © 2023 Pandey et al. This is an Open Access article distributed under the terms of the Creative Commons Attribution 4.0 International License (CCBY) (http://creativecommons.org/licenses/by/4.0/) which permits commercial use, including reproduction, adaptation, and distribution of the article provided the original author and source are credited.

Published by United Scientific Group

Abstract

The physical properties and spray performance of aviation fuel were examined in relation to the dispersion of nanoparticles. In order to achieve this goal, various weight concentrations of silicon dioxide (SiO_2) nanoparticles are studied in relation to the traditional Jet A-1 aviation fuel. The base fuel (BF) and nano fuels (NF) were measured for their important physical parameters like density, surface tension, and viscosity, which are crucial for the fuel atomization process. The shadowgraph method is used to find the macroscopic spray characteristics, such as the spray cone angle and the sheet breakup length. Utilizing the phase Doppler anemometry (PDA) approach allows for the measurement of the tiny spray properties, including droplet diameter, velocity, and distributions. Two injection pressures, 0.4 MPa and 1.2 MPa, are used to test the spray performance. The results demonstrate that the fuel's density and viscosity rise as the concentration of nanoparticles in the BF increases, while the surface tension falls. The effect of increasing nanoparticle concentrations on spray performance is a shortening of the liquid sheet breakup length. In addition, compared to the BF, NF has smaller mean droplet sizes.

Keywords

Phase Doppler anemometry, Nano fuel properties, Sheet breakup length, Silicon dioxide nanoparticles, Spray characteristics

Introduction

Research has shown that incorporating highly energetic materials like silicon (Si), boron, and iron into slurry fuels, which are liquid fuels with a high concentration, in sizes ranging from multiple micrometers, enhances their energy content [1, 2]. The metal particles in slurry fuels were claimed to cluster together, delaying ignition, which was the main issue with burning these fuels [3, 4]. When added to liquid fuel, this component negated the beneficial impact of energetic components on combustion efficiency.

Several energy-saving uses and unexpected improvements in thermophysical properties have piqued the interest of researchers in nanofluids, which are solutions comprising a diluted combination of particles with a size of less than 100 nm [2]. Based on this principle, there has been recent interest in NFs, which are fuels combined with energetic metal nanoparticles, due to their improved combustion characteristics. Catalytically increasing the burning rate, decreasing pollutants, and shortening the ignition delay are all outcomes of adding metal nanoparticles to liquid fuels. To get around the problem of extended ignition

delays and obtain greater burn rates, energetic metal particles have been shrunk from micrometers to nanometers [5, 6]. Particles on the nanometer scale are more desirable than their micrometer-sized equivalents due to their large surface area and the possibility of energy storage on the surface. Due to its high combustion enthalpy and cost-benefit analysis, silicon has been the most extensively utilized metal among other energetic particles. Recent studies have focused on examining the auto-ignition and combustion characteristics of heat transfer efficiency, specific heat, evaporation, and SiO_2 nanoparticles in aircraft turbine fuel [7, 8]. Adding Si/SiO_2 nanoparticles to fuel for aircraft turbines improved its performance in every single study. The study also investigated the impact of Si/SiO_2 nanoparticles on the physical properties of the fuel, including viscosity and surface tension [9, 10]. There was a 20% increase in fuel viscosity when SiO_2 nanoparticles were disseminated in aircraft turbine fuel at a 1% volume concentration. Nevertheless, there were conflicting findings when measuring the surface tension of nanofluids. While some research [11, 12] found that particle loading increased surface tension, other studies found the opposite—a drop at lower concentrations followed by an increase at higher loading levels. While some research revealed that the addition of particles enhanced surface tension, other investigations revealed the contrary to be true: Surface tension was shown to decrease at lower concentrations and then increase as particle loading increased [13, 14].

It is important to remember that as NFs' physical attributes change, it may also affect how they atomize, which in turn affects how they mix, burn, and emit. Thermophysical qualities, evaporation, combustion, and emission characteristics have been the primary foci of most research on NFs, especially those utilized in aviation. There has been a lack of research on how nanoparticles affect the spray performance of fuels used in aircraft turbines. To fully grasp the benefits of NFs, one must have a deeper comprehension of their atomization properties, since atomization plays a pivotal part in the subsequent processes. The current work is inspired by this.

One of the main goals of this study is to find out how spray performance at ambient atmospheric conditions is affected by SiO_2 nanoparticles mixed into regular Jet A-1 aviation fuel. The density, surface tension, and viscosity, among other physical parameters, are assessed since they are important for the atomization process. At two distinct injection pressures, the spray properties of NFs and BF are studied. The impact of nanoparticles will be demonstrated by comparing the outcomes of NFs with those of the BF. The shadowgraph approach is utilized near the nozzle to analyze the macroscopic spray features, including the length of the sheet breakup and spray cone angle. The PDA method is utilized to detect microscopic spray properties like droplet diameter and velocity dispersion.

Methodology

The technology utilized to manufacture the NF, the tools for analyzing its physical characteristics, the spray testing facility, and the optical testing methods applied to the spray are all detailed below.

Preparation of NF

The nanoparticles in this investigation were suspended in Jet A-1 fuel, which served as the BF. NFs were produced by dispersing SiO_2 particles (27 - 43 nm) of commercial origin in concentrations of Jet A-1 fuel ranging from 1 - 6 wt.%. The SiO_2 powder was subjected to energy dispersive X-ray spectroscopy analysis prior to preparing the sample, which revealed a high degree of chemical purity and the absence of any other elements. This allowed for the assessment of the quality of the nanoparticles.

Without the use of any stabilizing chemical agent, nanoparticles were disseminated in Jet A-1 fuel sample as the initial stage in the production of NFs (called as the surfactant). But it just took two minutes for the nanoparticles to settle to the bottom. Consequently, not even after two hours of strong sonication was a stable NF able to be produced. In conclusion, a nonionic surfactant was employed to stabilize NFs. According to reports, adding surfactant lowers the nanoparticles' surface energy, which in turn lowers the attraction interactions between the particles, which in turn reduces agglomeration [15]. An independent stability investigation was undertaken in iterations to determine the necessary amount of surfactants required to produce a stable NF sample. NF samples were placed in burettes with various concentrations of surfactants to visually assess sedimentation rates and stability. In order to create a stable, uniform NF, the results of the stability research dictated that 0.5% surfactant (by volume) should be added to the base fluid. From now on, the phrase "BF" will denote a combination of the surfactant and pure Jet A-1 fuel.

Nanoparticles were added to the Jet A-1 fuel after the surfactant had been blended with it at the specified weight percentage. A uniform and stable NF was created by exposing the mixture in a beaker to repeated cycles of ultrasonication for around 1 h. The process included 10 sec of sonication and 5 sec of idle time utilizing a probe-type sonicator. A heat exchanger was utilized to maintain a controlled temperature environment and prevent the production of fuel vapor during the NF sonication process. Consistent with the stability investigation, the NFs were subjected to sonication. The trials showed that the NF at its highest concentration remained stable for almost 4 h. A small amount of nanoparticle sedimentation was noted after 4 h. Instead of using a protracted period of sonication, light shaking was sufficient to return the NFs to a stable, homogeneous form. In terms of stability, adding more sonication time wasn't much different from the surfactant effect [16]. Verifying that the BFs chemical properties are unaffected by the surfactant addition is also crucial. The BF and NF had chemical properties like pure Jet A-1 fuel due to their low levels of surfactant and nanoparticles.

Property measurements

An lVISC viscometer was used to measure the NF samples' viscosity. The viscosity of the flow through a rectangular microchannel is determined in this configuration by measuring the pressure drop. The channel's small size allows for the detection of viscosity at high rates of shear, typically in spray applications. The viscosity data provided here is precise, with a shear range of 1000 – 7650 s^{-1} and accuracy

of 60.006 cP. Using the conventional methods of measuring volume and weight, we were able to ascertain the BFs density. Another option was to use the normal mixture methods to determine the NFs' density, given that the mass of the injected nanoparticles. Pure Jet A-1 fuel has a density of 0.788 g/cm^3.

The Kruss DSA 25 drop analyzer was another method employed to measure the surface tension of the NF samples. The surface tension was determined by analyzing the interfacial tension and the opposing gravity force acting on the surface of a hanging droplet, which is shaped by this balance. Based on the droplet's shape, the surface tension was then calculated using the Young-Laplace equation. Repeatability was maintained within 61% across all metrics, which were subjected to many trials. A refractometer, namely the RE40D model made by MettlerTeldo and located in Columbus, OH, was used to measure the NFs' refractive indices. This particular model is based on the total internal reflection principle. An accuracy of 60.002 was achieved in measuring the refractive index values that are presented here.

Spray testing facilities

Figure 1 is the schematic view of the experimental setup that was utilized in this study. To pressurize the fuel within the fuel chamber, we utilized nitrogen gas that was recovered from the cylinder, which is at a greater pressure. A two-way solenoid valve was used to manage the fuel flow to the nozzle at the specified injection pressure. The computer's transistor-transistor logic signals were used to synchronize the 2-way control valve with the camera. A pressure transducer was placed just upstream of the nozzle to continually measure the injection pressure. The features of the optically accessible spray chamber that was employed in this investigation have already been published elsewhere [17]. This study utilized a pressure nozzle as its atomizer. It had an outlet diameter of 0.8 mm and a flow number of 4.56 lb h1/(psid)0.5. The fuel vapor produced throughout the trials was continuously drained out of the spray chamber through the vapor exhaust situated at its base in order to prevent vapor saturation within.

In order to ensure good reproducibility, experiments were carried out three times for each example. Prior to switching between fuel samples, the fuel delivery system was drained of its fuel. After that, the system was dried using nitrogen gas and flushed with pure Jet A-1 fuel. The NF concentration was not affected by following this process, which was used to eliminate any traces of nanoparticles stuck within the tubes.

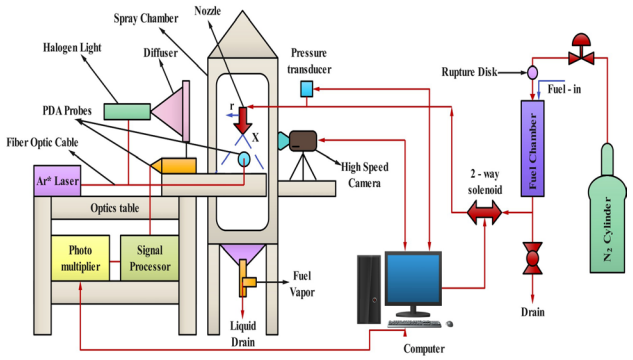


Figure 1: Diagram of the PDA transmitter and receiver probe-integrated spray experimental setup.

Spray optical diagnostic techniques

Optical diagnostic methods were used to measure the macroscopic and microscopic spray characteristics. For the macroscopic analysis, the shadowgraph method was employed to record the local nozzle parameters that influence the ignition probability in a real combustor, including liquid sheet breakup length and spray cone angle. The microscopic characteristics of the spray, including its velocity, droplet size, and dispersion downstream of the nozzle exit, influence the fuel location inside the combustors. However, these elements can be better understood utilizing the PDA method.

The experiment's light source was a 150 W halogen bulb attached to the spray's side. To prevent light from directly hitting the glass wall of the spray chamber, a diffusing screen was positioned between the two. Having a pixel resolution of 512 x 512, every image included a radial distance of about 18.5 mm following nozzle departure. A common calibration target utilized in particle image velocimetry and other velocimetry measures was used to calibrate the field of view and generate the factor for converting image coordinates to actual ones.

A 2D PDA system was utilized to measure the size and velocity of droplets at specific points simultaneously. In the PDA measurement method, the diameter of the droplet is estimated by comparing the two Doppler burst signals it emits as it moves across the measuring volume and finding the phase shift disparity. In this study, the first-order refraction Doppler signal was collected in forward-scatter mode with the receiver probe angled at 42°. The size and velocity of the droplet were then ascertained by processing the data using a signal-processing unit. Table 1 shows the summary of the PDA system's operational parameters.

The PDA measurements were conducted on only one side of the spray since it was symmetrical around the nozzle axis. Later on, the rationale behind selecting this axial site will be clarified. From the axis of the nozzle outward to the spray periphery, radial measurements were taken at 6-mm intervals. At each radial point, we measured up to five thousand samples or ten seconds in order to collect droplet readings that were

Table 1: 2D PDA system operating variables.

Operating variables	Units	
Measurement volume		
Length (dz)	mm	3.97
Diameter (dx)	μm	189
Fringe spacing	μm	5.27
Number of fringes	-	36
Receiving optics		
Scattering angle	Degree (°)	42
Focal length	mm	500
Aperture mask	-	Mask-B
Transmitting optics		
Beam spacing	mm	38
Focal length	mm	400
Beam waist	mm	1.35

statistically independent. Every radial point was tested three times. In addition, the size and velocity characteristics of the NF droplets were only assessed for the 3 wt.% concentration. This is because the 6 wt.% case's PDA measurements could not be confirmed because the fuel sample was visibly thicker than the 3 wt.% instance.

Results and Discussion

Here we detail the findings from the physical parameter measurements of the BF and NFs. The spray properties of the BF and NF were analyzed based on measurements obtained at injection pressures of 0.4 and 1.2 MPa. The surfactant and pure Jet A-1 fuel used together are referred to as BF. Except when otherwise noted, the error bars depict the usual standard deviation at an 85% confidence level for the data that is provided.

NF Properties

Figure 2a displays the viscosity of the BF and NFs changing with shear speeds. Both the base fuel and the NFs exhibit Newtonian behavior at the shear rates that have been measured. The expected relationship between the nanoparticle concentration and fluid viscosity is illustrated in this figure. The 6 wt.% case shows the highest rise, with a viscosity that is 2.5% higher than the standard fuel. These trends are in line with the conventional effective medium theory for mixtures and are consistent with what is seen in the research [18]. Figure 2b shows a comparable pattern for the fuel density change as a function of nanoparticle concentrations.

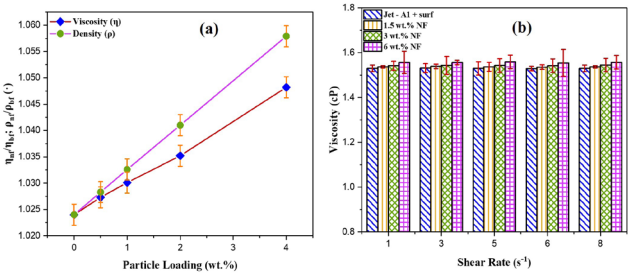


Figure 2: (a) Viscosity and density ratio and **(b)** Viscosity variation with shear variation of NFs.

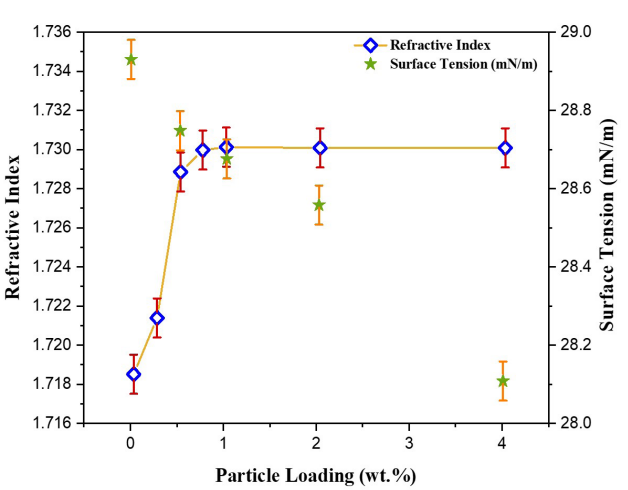


Figure 3: Computation of NFs' surface tension and refractive index.

Both NFs and BF show variations in surface tension and refractive index in figure 3. Particle loading has a negligible effect on the refractive index readings. This remains unchanged even when adding particles to a maximum of 6 wt.%. In addition, after 1.5 wt.% particle loading, the refractive index doesn't change substantially. It is desirable that there be little variation in the refractive index value when comparing NFs to the BF, since this will lead to optical measurements with almost little uncertainty. It is noted that when the particle loading increases, the surface tension values decrease. This effect could be caused by the use of a surfactant during the preparation of NFs, in addition to particle effects. Reportedly, the decrease in surface tension is due to the surfactant-induced accumulation of nanoparticles at the gas-liquid interface. While NFs' surface tension drop is negligible in comparison to the BF, it might have a significant impact on spray characteristics.

Spray characteristics

Here we give and debate the NF's and BF's spray performance. Because NF opacity rises with particle loading, NFs with smaller particle weight concentrations of 1, 1.5, and 3 wt.% are chosen for the spray characteristics investigation. To emphasize the impact of nanoparticle concentrations, the outcomes are contrasted with the BF's. Two parts follow, each devoted to a different aspect of the spray's micro and macro details.

Visualization of spray

The angle of spray cone influences the ignition probability in real combustors, making it a crucial characteristic for pressure nozzle applications. In contrast to fuel viscosity, which is a weak effect of the swirl chamber features of the nozzle strongly determines the angle of spray cone. According to predictions, the spray cone's angle is not affected by many fluid properties, including density and surface tension [19]. Finding the angle of spray cone, however, is necessary for ascertaining whether the nanoparticles exert any influence throughout spray production and stable operation. After running the shadowgraph images through an edge recognition algorithm, we can determine the spray cone angle and, by implication, the spray edges (2h). Figure 4 displays the initial shift in the spray cone angle as the fluid exits the nozzle at time t = 0. In around 30 ms, the spray cone angle stabilizes for both the NFs and the BF. Among the examples tested, the NF spray with a 3 wt.% particle loading reached steady state at both injection pressures more rapidly than the others. Although this effect

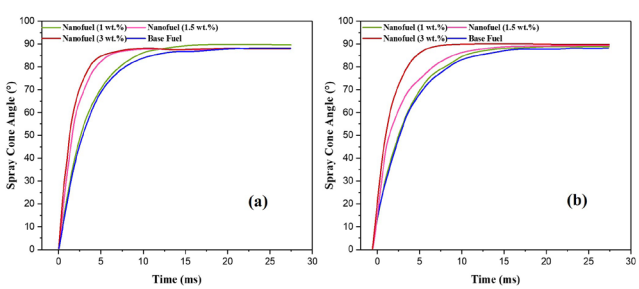


Figure 4: Changes in the angle of spray cone during the brief period of time.

is minimal at lower particle loadings, all NFs do attain steady operation at 1.2 MPa, which is slightly earlier than the BF. Base fuel and NFs have a slightly different viscosity, but the reason behind this difference is unclear because the swirl chamber parameters are unknown. The spray cone angle is calculated by analyzing approximately 20,000 shadowgraph images while the operation is steady (t > 60 ms). Assuming a continuous spray, the spray cone angle for NFs and BF falls within the range of 86 to 63°.

Because of its critical role in dictating the size and dispersion of the droplets, atomization properties such as sheet breakup distance are determined alongside the spray cone angle. A liquid sheet can disintegrate for at least two reasons, such as when disturbance waves dominate the surface of the sheet or when holes are punched into the liquid.

The duration of the sheet disintegration is determined by analyzing around 40 photos with a 50 ms interval between each one. An in-house MATLAB application is utilized for image processing in order to ascertain the sheet breakup length. The graphic uses a consistent arrow length across images to depict the sheet breakup distance in various conditions for simpler comparisons. Figure 5 demonstrates that for both injection pressures, the length of time it takes for the liquid sheet to break apart reduces as the concentration of nanoparticles increases. The time it takes for a sheet to break up can be affected by a number of variables, including changes in the fuel's viscosity and the relative velocities of the liquid and air. The fluid viscosity of the NFs may be the reason for the shortening of the liquid sheet breakup length when nanoparticles are added, given that the injection pressure remains constant throughout all of the fuels. It should also be noted that the proximity of the holes to the nozzle output increases as the concentrations of nanoparticles rise.

Comparing the properties of microscopic sprays

Parameters of the spray at the microscopic level, including the size of the droplets and their velocity as they travel in the radial direction, are addressed here. From a combustion standpoint, these characteristics matter because they dictate where the fuel is placed within the combustion chambers.

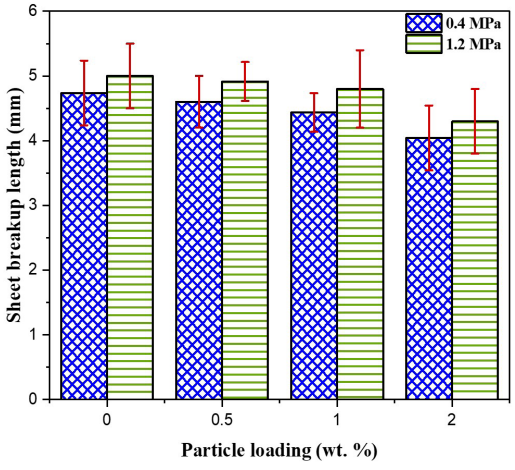


Figure 5: Varied lengths of liquid sheets that break up NFs and BF.

Injecting NF and BF droplets through the nozzle at two distinct pressures (0.4 and 1.2 MPa) allows the PDA method to assess their respective features, as previously stated. A single axial point 30 mm downstream of the nozzle output is the sole one where the droplet properties are studied. By leveraging the increased data rate of the different samples, this data rate is become nondimensional to make comparisons easier. At 6 mm intervals along the radial distance between the spray perimeter and the nozzle axis, radial PDA measurements are required for NFs.

Figure 6 displays the fluctuation of the arithmetic mean droplet diameter with varying injection pressures. The BF has mean droplet sizes that are approximately 3 to 6 µm larger than the NFs at 0.4 MPa, regardless of the radial location. The NFs showed reduced sheet breakdown lengths in comparison to the BF, as previously stated. Because of this, the NF droplets have more time to go through secondary atomization. Alternatively, along the nozzle axis, NFs have somewhat larger mean diameters at 1.2 MPa, which drop below the base fuel at r = 12 mm and beyond. Strangely, the disparity between the NF and BF's mean droplet diameters increases as one travels outward in the radial direction. Continuous and dashed lines, which reflect second-order polynomial fits, indicate the trends.

Figure 7 compares the data rate patterns of the NF and BF to gain further insights into this trend. Displayed on separate scales are the data rate characteristics for the 0.4 MPa and 1.2 MPa instances to make comparisons easier. In the case of reduced injection pressure, the data rate profile matches the trend in mean droplet diameter, as one would expect in a scenario with a shorter breakdown period. Data rates are significantly lower than BF levels regardless of the length of the sheet breakdown. This suggests that there is a

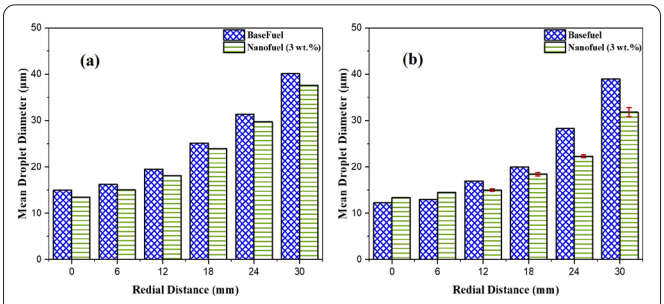


Figure 6: At 0.4 and 1.2 MPa injection pressures, the BF and NF (3 wt.%) show mean radial diameter variation at x5 30 mm.

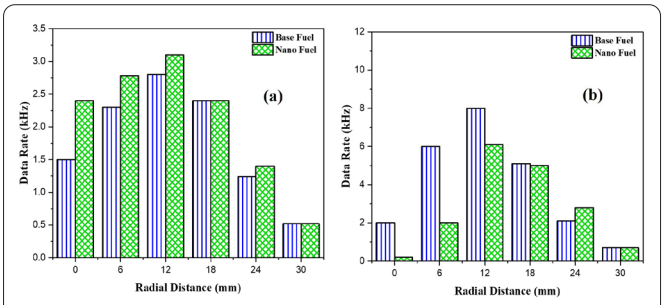


Figure 7: x5 30 mm radial profiles of data rate for NF and BF (3 wt.%) at 0.4 and 1.2 MPa pressures of injection.

discrepancy between the rate of data characteristics for the trend for minimum injection pressure and scenario with maximum injection pressure in the 0 < r < 18 region. In the area around the spray's periphery, nevertheless, the NF's data rates are either higher than or on par with the BF's. In the spray perimeter zone (0 < r < 18), there is a potential for an opaque layer of droplets to alter the Doppler bursting signals from the measured volume, potentially affecting the measurement instrument's accuracy. The data rate patterns of NF and BF are similar, with the most significant difference in mean droplet sizes occurring at radial points greater than 18 mm.

In addition, figure 8 compares the Sauter mean diameter, which is important for combustor design and is the ratio of the droplet's volume to its surface area. When the injection pressure is lowered, the BF and NF are quite similar with respect to the Sauter mean diameter. At higher injection pressures, the NF always has Sauter mean diameters that are around 7 μm smaller than the base fuel. One more way to compare NF to the BF is to look at their mean axial droplet velocity, as shown in figure 9. The disparity between the fuels' mean axial droplet velocities shrinks as the radial distance from the injection point increases under reduced injection pressure. The reason behind this could be that the NF causes the droplets to move at a somewhat faster speed compared to the BF. The discrepancy in mean droplet velocities between the BF and NF is constant across all radial regions when the injection pressure is increased. Because NF droplets are much smaller than BF droplets, they are able to travel with a higher momentum.

The data clearly show that nanoparticles affect the spray's macroscopic and microscopic properties, even if the nanoparticle weight percentages are lower than the combustion tests reported in the research. Additionally, modest particle loading concentrations would be beneficial since they wouldn't mess with the engine's other mechanical system design. The nanoparticles can substantially affect fluid characteristics at high particle loading, leading to an alteration of spray features.

Conclusions

An extensive investigation was conducted to determine the impact of nanoparticle dispersion on the spray characteristics of Jet A-1 aviation turbine fuel. This was accomplished by measuring the NF and BF for physical parameters relevant to the atomization process, including density, surface tension, and viscosity. As the concentration of nanoparticles in the gasoline grew, the density and viscosity could only rise by 3%. Nanoparticle dispersion in Jet A-1 fuel had a negligible effect on surface tension and refractive index.

During the transient period of the spray, it was found that the NF and BF had different spray cone angles, even though their viscosity was almost irrelevant. A key component in determining droplet properties, the sheet breakup length, decreased as the nanoparticle amount increased. On top of that, the nozzle exit was the spot where the perforations on the surface of the liquid sheet were most noticeable. Thus, the liquid sheet for the NFs disintegrates more quickly than the BF. NF consistently had smaller mean droplet sizes than the

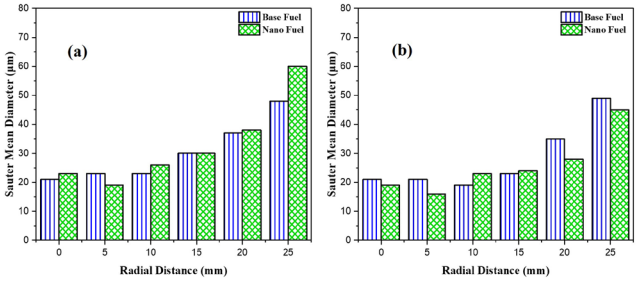


Figure 8: At 0.4 and 1.2 MPa injection pressures, the radial variation in the Sauter mean diameter of the NF and BF (3 wt.%) is at x5 30 mm.

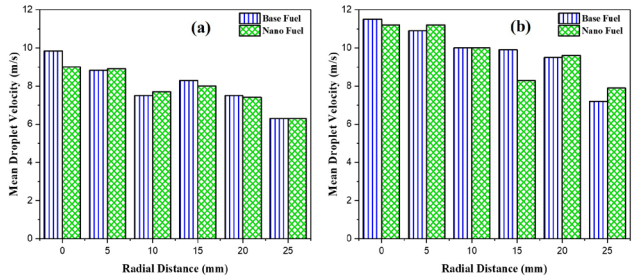


Figure 9: Analysis of the NF and BF (3 wt.%) injection velocities at 0.4 and 1.2 MPa along the radial direction at x5 30 mm.

BF. This may be because the NFs' liquid sheets disintegrate more quickly, leaving more time for secondary atomization. When contrasted with the BF, NFs showed higher mean axial droplet velocities. The reason behind this might be that the NF droplets are travelling at a higher momentum than the higher droplets in the BF instance.

All of these readings point to the fact that nanoparticles had an obvious impact on the spray characteristics despite the low concentrations. Some research in the literature has shown that this impact can become even more pronounced with a much greater concentration of nanoparticles. The real benefits of NFs in real combustor circumstances might be better understood with additional research on spray properties.

Acknowledgements

None.

Conflict of Interest

None.

References

1. Muduli SK, Mishra RK, Mishra PC. 2023. Computational assessment of performance parameters of an aero gas turbine combustor for full flight envelope operation. *Int J Turbo Jet Engines* 40(4): 481-491. https://doi.org/10.1515/tjj-2021-0034
2. Zha K, Busch S, Warey A, Peterson RC, Kurtz E. 2018. A study of piston geometry effects on late-stage combustion in a light-duty optical diesel engine using combustion image velocimetry. *SAE Int J Engines* 11(6): 783-804. https://doi.org/10.4271/2018-01-0230
3. Cohen AY, Sattarov A, Claramunt K, Anker JE, Romagnosi L, et al. 2023. Simulation and analysis of an aero-engine combustor with a slinger fuel injection system. *Int J Turbo Jet Engines* 40(2): 193-201. https://doi.org/10.1515/tjj-2020-0044

4. Sciortino DD, Cary M, Verma S, Biagiotti F, Hopkins E, et al. 2021. Development of a PN surrogate model based on mixture quality in a GDI engine. *SAE Tech Paper* 1-12. https://doi.org/10.4271/2021-24-0013
5. Vacca A, Hummel S, Müller K, Reichenbacher M, Chiodi M, et al. 2020. Virtual development of injector spray targeting by coupling 3D-CFD simulations with optical investigations. *SAE Tech Paper* 1-17. https://doi.org/10.4271/2020-01-1157
6. Aljure A, Tauzia X, Maiboom A. 2018. Heat release rate modeling improvement in an eulerian 1D diesel combustion model. *SAE Tech Paper* 1-15. https://doi.org/10.4271/2018-01-1127
7. Azam Q, Sulaiman SZ, Abd Razak N, Mazlan NM. 2023. Spray behaviour of hydro-treated ester fatty acids fuel made from used cooking oil at low injection pressures. *Aeronautical J* 1-15. https://doi.org/10.1017/aer.2023.80
8. Wadekar S. 2019. Large-eddy simulation on the effects of fuel injection pressure on gasoline spray characteristics. Chalmers Tekniska Hogskola. (Doctoral Dissertation)
9. Wadekar S. 2019. Investigation of Influence of Injection Pressure on Gasoline Fuel Spray Characteristics Using Numerical Simulation. In Singh A, Shukla P, Hwang J, Agarwal A (eds) Simulations and Optical Diagnostics for Internal Combustion Engines. Energy, Environment, and Sustainability. Springer, Singapore, pp 69-83.
10. Fujiwara T, Suematsu K, Okazaki T, Kobayashi Y, Suehiro K. 2023. Effects of throat shape on combustion improvement in a swirl-chamber diesel engine with electronically controlled multi hole injector. *SAE Tech Paper* 1-8. https://doi.org/10.4271/2023-01-1819
11. Sharma N, Agarwal AK. 2021. Macroscopic spray characteristics of a gasohol fueled GDI injector and impact on engine combustion and particulate morphology. *Fuel* 295: 120461. https://doi.org/10.1016/j.fuel.2021.120461
12. Tariq AI, Saleh AM. 2023. An experimental investigation into the combustion properties, performance, emissions, and cost reduction of using heavy and light fuel oils. *Case Stud Therm Eng* 44: 102832. https://doi.org/10.1016/j.csite.2023.102832
13. Yilmaz E, Suzuki T, Ito K, Gotama GJ, Anggono W, et al. 2021. Analysis of the spray characteristics of water and water/glycerin mixtures using an interferometric laser imaging for droplet sizing technique. *Int J Technol* 12(1): 101-112. https://doi.org/10.14716/ijtech.v12i1.4188
14. Anufriev IS, Kopyev EP, Sadkin IS, Mukhina MA, Minakov AV, et al. 2023. Combustion of n-heptane with steam injection in a laboratory spray burner. *Thermophys Aeromech* 30(2): 249-262. https://doi.org/10.1134/S0869864323020063
15. Sudarmanta B, Mahanggi AA, Yuvenda D, Soebagyo H. 2020. Optimization of injection pressure and injection timing on fuel sprays, engine performances and emissions on a developed DI 20C biodiesel engine prototype. *Int J Heat Technol* 38(4): 827-838.
16. Yadav PS, Chaturwedi AA, Sahu A, Yadav A, Fraynjiya A, et al. 2023. Effect of Nozzle Geometry and Fuel Modification on Atomization and Emission Characteristics in CI Engine: A Review. In Li X, Rashidi MM, Lather RS, Raman R (eds) Emerging Trends in Mechanical and Industrial Engineering. Lecture Notes in Mechanical Engineering. Springer, Singapore, pp 13-32.
17. Gamertsfelder J, Khare P, Bravo L. 2020. Investigation of atomization behaviors of liquid monopropellants in pintle injectors. In Proceedings of ASME Turbo Expo: Power for Land, Sea, and Air, Virtual.
18. Buss L, Bianchi Neto P, França Meier H, Noriler D, Fritsching U. 2018. Temperature distribution in open and enclosed flame spray reactor. In 14th Triennial International Conference on Liquid Atomization and Spray Systems, Chicago, IL, USA.
19. Pan L, E X-T-F, Cao J, Xue K. 2020. Design and Synthesis of Nanofluid Fuels. In Zou J-J, Zhang X, Pan L (eds) High-Energy-Density Fuels for Advanced Propulsion: Design and Synthesis. Wiley-VCH GmbH, pp 291-375.